

Full Length Research Paper

Calculation and analysis of pore vapor pressure of concrete exposed to fire

Min Li^{1,2*}, Zhishen Wu², Hongtao Kao³, Chunxiang Qian¹ and Wei Sun¹

¹Jiangsu Province Key Laboratory for Construction Materials, Southeast University Nanjing 211189, China.

²Low-Carbon Building Environment Equipment and System Energy-saving Engineering Center of Education Ministry, Southeast University, Nanjing 211189, China.

³School of Materials Science and Engineering, Nanjing University of Technology, Nanjing 210009, China.

Accepted 23 June, 2010

The present work involves calculation and analysis of pore vapor pressure in high strength concrete (HSC) exposed to fire. In order to study the spalling of high strength concrete exposed to fire, a mathematical model of the coupled actions of hydro-thermal effects is established. The temperature field and the pressure field are calculated at a given temperature. Then, the pore vapor pressure is calculated and analyzed and the calculated results are validated experimentally. The relationships between the water permeability coefficient or the vapor permeability coefficient and the peak pressure together with its location are established. The results from this study indicate that peak pore pressure increases with prolonged fire exposure time and shifts from the surface towards the center of the concrete. The research results provide a basis for improving the spalling phenomenon.

Key words: High strength concrete, coupling of water vapor and heat, pore pressure, water permeability coefficient, vapor permeability coefficient.

INTRODUCTION

High strength concrete is a brittle material that has low porosity and little water absorption. The water in concrete exists in the form of combined water, adsorbed water and free water. Compared with normal strength concrete (NSC), high strength concrete has low permeability, which reduces the rate at which water can be released. Several researchers have put forward various mechanisms to explain spalling of concrete exposed to fire, for example, thermal incompatibility, vapor pressure and thermal stress. High temperatures can cause the water in the pore space of the concrete to vaporize, increasing the pressure in the pores and inducing spalling on the exterior surface (Aitcin, 1989). Some research results show that high temperature induces thermal stress between the exterior layer and the interior of concrete, leading to spalling (Jahren, 1989). Other results show that hydrolysates of cement decompose at high temperature and release vapor, consequently the pore pressure increases and the paste matrix fractures (Phan, 1996).

Bazant (1979) analyzed hydro-thermal transfer in concrete and calculated the vapor pressure by finite element analysis. Kalifa et al. (2001) measured the vapor pressure in the interior of concrete and the results validated the theory of vapor pressure-induced spalling. Van der Heijden et al. (2007) studied fire spalling in concrete exposed to fire through measuring the moisture transport in heated concrete using the dedicated nuclear magnetic resonance (NMR) method. Mindeguia et al. (2010) used a device intended for measuring temperature and pore vapour pressure of concrete specimens. The aim of the study was to better understand the thermo-hydral behaviour of concrete exposed to high temperature and the possible link to spalling risk.

Spalling of concrete exposed to fire is the result of a combination of heat-related and vapor-related effects. On one hand, a temperature field arises from external heating and internal heat transfer and results in a thermal expansion gradient grade and tensile stress that is perpendicular to the fire-exposed surface. On the other hand, the effects of mass transfer (for example, water, vapor and air) in a porous media can lead to internal pressure, resulting in a "homothetic saturated zone." Because of the coupling between the combined

*Corresponding author. E-mail: limin.li@163.com.

hydrothermal effects, stress and strain are imposed that lead to spalling.

There are many mathematical models based on different spalling mechanisms. Other researchers have developed thorough studies on simulations of the permeability of cementing materials, numerical simulations of hydro-thermal conduction and modeling mass transfer in the interior of concrete (Wittmann and Schweisinger, 1998; Johannesson, 2002). Many researches in this field are concerned with analyzing the temperature field in the interior of concrete exposed to fire, while there is very little investigation of the internal vapor pressure field. In this paper, a mathematical model of the coupled hydro-thermal effects is established. The temperature field and pressure field are built and calculated for a given temperature exposure. Then, the pore pressure is calculated and analyzed and the calculated results are verified experimentally.

MATHEMATICAL MODEL OF HYDRO-THERMAL EFFECTS

As a reasonable simplification, ideal conditions are assumed as follows:

- (1) Concrete is isotropic and homogeneous.
- (2) Concrete is completely mature, so there is no hydrate reaction in the concrete and concrete is saturated at normal temperature.
- (3) In the pores of the concrete, there is only vapor pressure, and the vapor is an ideal gas.
- (4) Only the pressure field in front of the "homothetic saturated zone" (Bazant, 1979) is considered.

Based on the above assumptions, the temperature field can be calculated from the diffusion equation:

$$\frac{\partial T}{\partial t} = \frac{k}{\rho C} \nabla^2 T \tag{1}$$

where k is the coefficient of thermal conductivity, ρ is density, C is specific heat, t is time and T is temperature.

The pressure field is regarded as a function of temperature (T) and mass density of vapor (w).

The state equation of an ideal gas is

$$pv = nRT \tag{2}$$

Where p is the pressure of the ideal gas, v is the volume, n is the molar amount, and R is the universal gas constant. In volume element dv, n is given by

$$n = wdv / M$$

Where M is the molar mass (0.018 kg/mol for water vapor).

So,

$$pdv = wdvRT / M \tag{3}$$

That is,

$$p = wRT / M \tag{4}$$

So, w is related to p by

$$w = Bp \tag{5}$$

Where

$$B = M / RT \tag{6}$$

The concentration gradient of vapor is the driving force of diffusion. Linear diffusion within concrete is given by:

$$J = -D \frac{\partial w}{\partial x} \tag{7}$$

where J is mass flux, D is the diffusion coefficient and x refers to the x-direction.

Neglecting any vapor sources, the mass equilibrium equations is

$$\frac{\partial w}{\partial t} + \nabla J = 0 \tag{8}$$

Combining Eq. (7) and Eq. (8), the following equation is obtained:

$$\frac{\partial w}{\partial t} = \nabla(D \frac{\partial w}{\partial x}) \tag{9}$$

In this model, diffusivity (D) is considered to be a variable because diffusivity increase with temperature. In this aspect, the model is new comparing to that of other research. Ichikawa and England (2004) assumed that the diffusion coefficient is $4.0 \times 10^{-9} m^2 s^{-1}$ in order to simulate the experimental data, which is different from the real situation.

An empirical formula for D (Equation 10) is given in the study of Yang Daiquan (Daiquan and Zhujiang, 2000). After damage induced by high temperature is considered, the coefficient of permeability must be corrected as in Equation (11) (Min, 2005).

$$D = 2.29 \times 10^{-5} (1 + \frac{T}{273})^{1.75} \tag{10}$$

$$D = 0.08346 e^{(T/426.21207)} \tag{11}$$

Equation (9) can be written as:

$$\frac{\partial w}{\partial t} = D \nabla^2 w + \frac{\partial w}{\partial x} \frac{\partial D}{\partial x} \tag{12}$$

Considering one-dimensional diffusion, Equation (13) is obtained by combining Equation (5) and (12)

$$\frac{\partial B}{\partial t} p + \frac{\partial p}{\partial t} B = D (\frac{\partial^2 B}{\partial x^2} p + 2 \frac{\partial B}{\partial x} \frac{\partial p}{\partial x} + \frac{\partial^2 p}{\partial x^2} B) + \frac{\partial D}{\partial x} (\frac{\partial B}{\partial x} p + \frac{\partial p}{\partial x} B) \tag{13}$$

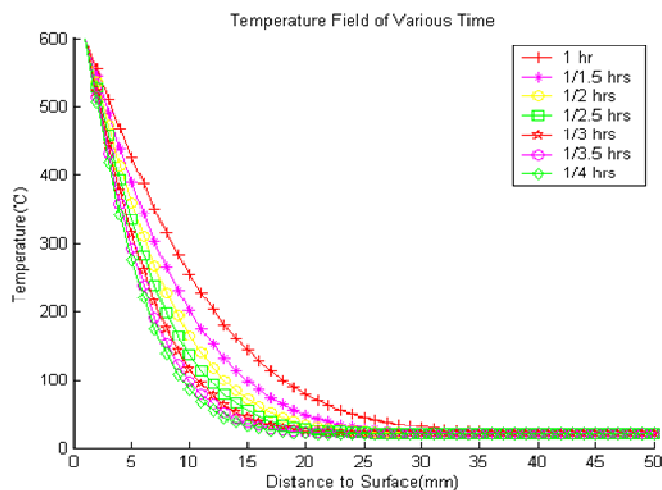
This partial differential equation is solved by the finite difference method and is calculated by using MatLab. The thermotechnical parameters of concrete are introduced into the calculations (Yuzhang, 1998):

$$\rho = 2350 \text{ kg/m}^3;$$

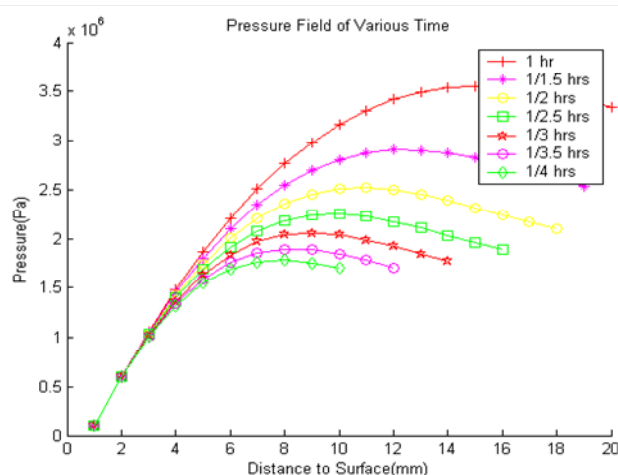
$$k = 2 - 0.24T/120 + 0.012 \times (T/120)^2;$$

$$C = 900 + 80T/120 - 4 \times (T/120)^2.$$

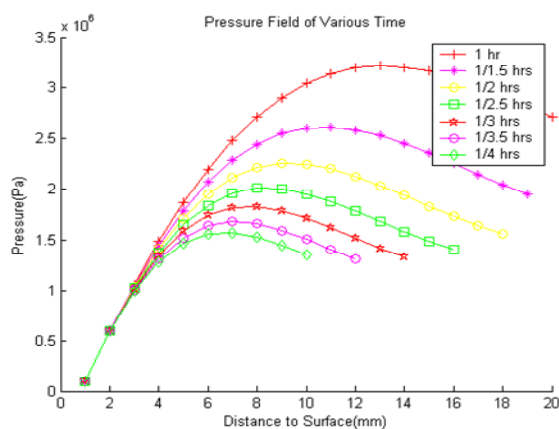
Figure 1 depicts the calculated results for the temperature field and pressure field. From Figure 1(a), it can be seen that the



(a)



$$(D = 2.29 \times 10^{-5} (1 + T/273)^{1.75})^{[8]}$$



$$(D = 0.08346 e^{(T/426.21207)})^{[9]}$$

(b)

Figure 1. The temperature field and pressure field at different heating time. (a) The temperature field. (b) The pressure field.

temperature distribution within the concrete is very non-uniform because of its poor thermal conductance. The surface temperature reaches 600°C when the concrete slab is heated at 600°C for 0.25 h, however, the temperature 20 mm from the fire-exposed face is only 25°C. With increasing fire exposure time, the temperature in the interior of the concrete increases very slowly. After the concrete slab is heated at 600°C for 1 h, the temperature in the center of the concrete slab is only 40°C. From Figure 1(b), it can be seen that there is a maximum value of pressure in the pressure field. This peak pressure increases with fire exposure time and the location of peak pressure gradually moves away from the fire-exposed surface.

Figures 2 and 3 show the relationship between the peak pressure and the fire exposure time and temperature respectively. Peak pressure increases linearly while the concrete continues to be exposed to fire, but the corresponding temperatures of peak pressure are all about 150°C. This temperature is near the melting point of polypropylene fiber (165°C), which can explain why polypropylene fiber can improve the spalling resistance of high strength concrete. At that temperature, peak pressure appears in certain locations in the concrete. After the polypropylene fibers melt, many coterminal pores are opened, which serves to release vapor pressure and avoid spalling. This result not only validates vapor pressure theory but also indicates the credibility of the model established in this study.

Some previous studies found that spalling usually happens within 30 min after fire exposure and the spalling depth is generally within 10 mm. Figure 2 shows that the peak pressure in concrete exposed to fire for 30 min is 2.5 MPa and the corresponding location is 10 mm from the fire-exposed surface. Contraction micro-cracks occur first, and if vapor pressure is high enough, micro-cracks will enlarge rapidly. In extreme circumstances, the surface will fail by spalling. After such damage occurs, the diffusion coefficient of vapor increases markedly and vapor pressure correspondingly drops, halting spalling. This explains why spalling usually happens within 30 min after fire exposure. Under appropriate conditions, spalling may recur on a new surface, but this will eventually stop as the water content of the concrete is decreasing continually.

The calculated results of the empirical formula Equation (10) (Daiquan and Zhujiang, 2000) and Equation (11) (Min, 2005) are appreciably different. The peak pressure calculated using Equation (11) is lower than that calculated with Equation (10) and the difference increases gradually with prolonged fire exposure time. The corresponding temperature of peak pressure calculated with Equation (11) is higher than that calculated using Equation (10). When fire exposure time is increased from 15 to 60 min, the difference in peak pressure changes from 0.2081 to 0.3200 MPa and the corresponding temperature of peak pressure changes from 23.39 to 61.42°C Equation (11) accounts for the increase of permeability caused by structural damage in high-strength concrete exposed to fire.

EXPERIMENTAL VALIDATION AND ANALYSIS OF CALCULATED RESULTS FOR PORE PRESSURE

Raw materials and experimental method

The concrete used in this study consisted of Portland cement conforming to 42.5 P 2, river sand with fineness modulus of 2.50, crushed basalt, fly ash with grade 1, high range water reducing agent and two different types of polypropylene fiber with lengths of 6 and 19 mm, marked as PS and PL, respectively. The chemical composition of cement and fly ash are listed in Table 1. The mix proportions and compressive strength at 28 days

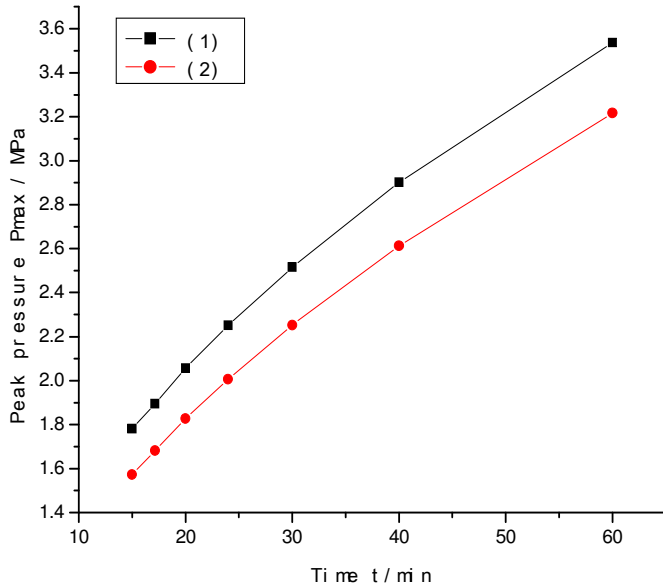


Figure 2. The relationship of peak pressure and fire exposure time of HSC. (1) ^[8]: $D = 2.29 \times 10^{-5} (1+T/273)^{1.75}$, (2) ^[9]: $D = 0.08346 e^{(T/426.21207)}$

of normal strength concrete (NSC) and high strength concrete (HSC) are listed in Table 2.

After being cured at 20°C and 90% relative humidity for 28 days, the specimens were placed in a normal temperature environment for 3 days. An oil furnace was used for the high-temperature tests. The sketch map of the oil furnace is shown in Figure 4. The furnace size is 580 × 400mm × 450 mm. The temperature-time curve of the oil furnace is near to the curve prescribed in ISO 834, which accords with Equation (14).

$$T - T_0 = 345 \lg(8t + 1) \quad (14)$$

Where T is the average temperature in furnace at the time of t, °C; T₀ is the initial temperature in furnace, °C; t is the heating time, minute.

When the temperature reached 600°C, the furnace was kept at constant temperature for 1 h, then heating was stopped and the specimens cooled to normal temperature inside the furnace.

Water absorption of high strength concrete exposed to fire was tested in order to confirm the relationship between water absorption and fire exposure time. The slope of the water absorption vs. time curve is the water permeability coefficient. This particular testing method is described in the study of Cemy and Rehalova (1996).

Validation of peak pore pressure

Figure 2 shows that the calculated value of peak pore pressure in concrete is about 3.5532 MPa after the concrete is exposed to fire for 1 h. If concrete cannot

endure this pressure, spalling will happen. The flexural strength and degree of spalling of HSC with PP fiber after 600°C are listed in Table 3. The flexural strength is tested from specimens without spalling, so the test results are roughly representative of the material's resistance to spalling. Table 2 shows that the flexural strength are decreased from 9.15 ~ 9.21 MPa to the ranges between 3.43 and 4.94 MPa, which is close to value of peak pressure. This result lends credence to the calculated results presented earlier.

Relationship of water permeability coefficient and peak pressure together with location of peak pressure

Vapor pressure comes into being in concrete pores at high temperature. It is very difficult to measure vapor pressure directly. The pore vapor pressure value can be confirmed by the temperature field and pressure field obtained in this study. On the other hand, the pore vapor pressure value can be confirmed by the water permeability coefficient, since the pore vapor pressure value is connected to the permeability of water and vapor in concrete. Relationships between water permeability coefficient and peak pressure together with the location of peak pressure are established in Figures 5 and 6. The value of peak pressure and its location are calculated, while the water permeability coefficient is obtained by experiment. The location of the peak pore pressure is denoted by its distance from the fire-exposed surface (that is, depth of pressure).

From Figures 5 and 6, it can be seen that there is a correlation between water permeability coefficient and peak pressure together with the location of the peak pressure.

The water adsorption can reflect the volume of pores in concrete. According to state equation of ideal gas, the pressure produced by evaporation of water in pores of concrete is inversely proportional to the volume of pores in concrete when temperature is a fixed value. So, the test of water adsorption can reflect the peak pressure at fixed temperature. The water permeability can be easily tested through the water adsorption test, so, the experiment validation through the water adsorption test is simple and convenient comparing to the method of measuring pore pressure that was described in the study of Kalifa et al. (2001).

Relationship of vapor permeability coefficient and peak pressure together with location of peak pressure

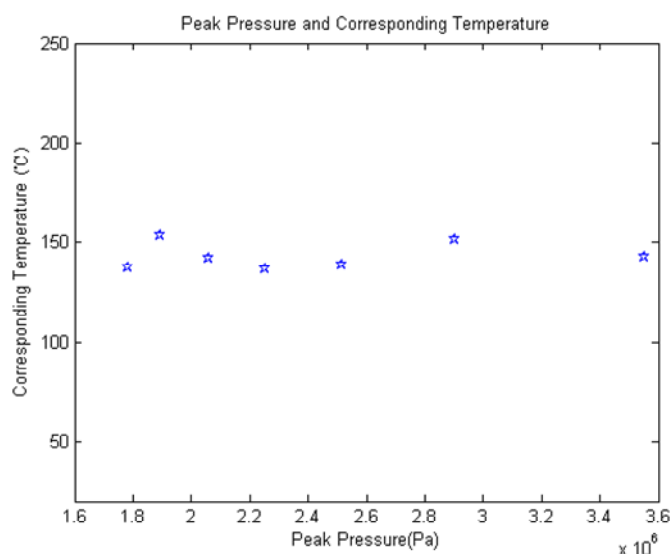
The permeability of concrete is very important in determining the pore pressure in concrete exposed to fire. If the concrete is more permeable, then the peak value of vapor pressure will be lower. Equation (11) indicates that

Table 1. Chemical composition of cement and fly ash

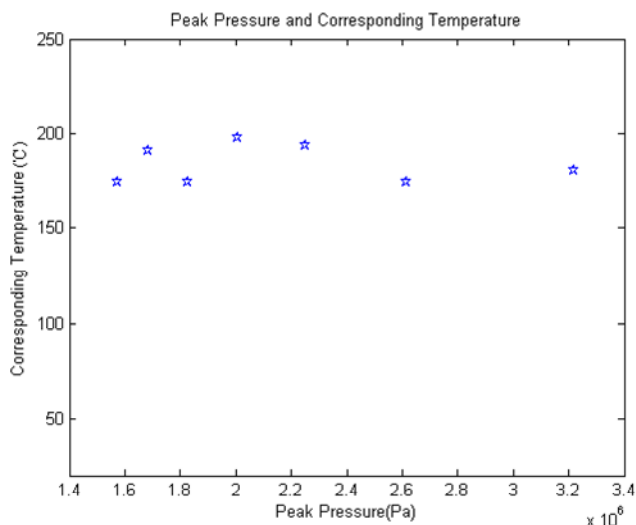
Chemical composition	CaO	SiO ₂	Al ₂ O ₃	Fe ₂ O ₃	MgO	Total
Cement / %	64.11	20.60	5.03	4.38	1.46	95.58
Fly ash/ %	57.66	29.84	2.29	5.85	2.52	98.16

Table 2. Mix proportions of concrete and compressive strength at 28 days.

Sample No.	Cement	Water	Sand	Aggregate	Fly ash	Water reducer	Compressive strength at 28 days
NSC-30	382	195	639	1184	—	—	39.8
HSC-50	327	144	638	1182	109	3.49	62.1
HSC-70	410	146	628	1116	150	4.10	82.3
HSC-90	450	138	581	1180	150	4.8	102.6



$$(D = 2.29 \times 10^{-5} (1+T/273)^{1.75}) \text{ [8]}$$



$$(Da = 0.08346 e^{(T/426.21207)}) \text{ [9]}$$

Figure 3. The relationship of peak pressure and corresponding temperature.

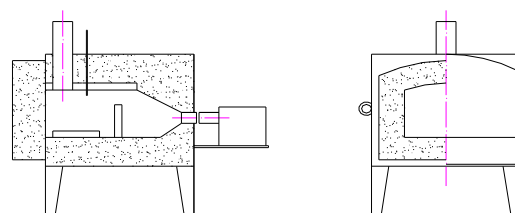


Figure 4. The sketch map of the oil furnace.

temperature appreciably influences the diffusion coefficient. Exposure to fire causes structural damage in concrete, so the vapor permeability coefficient increases and the peak pore pressure and its location consequently change.

The peak pore pressure and its location at a certain temperature are calculated using the MatLab program developed in this study, and then the vapor permeability coefficient at corresponding temperatures is obtained from Equation (10). Figure 7 shows the relationship of the vapor permeability coefficient and peak pore pressure and the depth of peak pressure.

After the temperature is ascertained, the vapor permeability coefficient in concrete is calculated using Equation (11). Thus, the peak pore pressure and depth of peak pressure at this temperature can be reckoned according to Figure 7. The vapor diffusion coefficient is treated as a function of temperature in this calculation, although it is also related to water content and other factors. It is very difficult to measure vapor pressure directly, so in order to estimate the pressure distributing in the concrete the water permeability coefficient, which can be measured easily, may be used for approximate calculations. This method is a practical way to assess spalling resistance.

Comparison of pore pressure for different concretes under high temperature

Pressure values in different kinds of concrete at 600°C are obtained by the relationship given in Figure 5. That is Equation (14).

Table 3. The residual flexural strength of HSC with PP fiber exposed to fire.

Sample no.	Content of PP fiber (kg/m ³)	The flexural strength at 25°C(MPa)	The flexural strength after 600°C(MPa)	Spalling degree (%)	Water permeability coefficient (kg/(m ² .s ^{1/2}))
PSV1	0.58	9.16	3.43	1.30	0.0946
PSV2	0.88	9.18	4.32	1.06	0.1162
PSV3	1.18	9.2	4.44	0.27	0.1429
PSV4	1.48	9.21	4.48	0.00	0.1521
PLV1	0.58	9.2	4.94	1.13	0.0962
PLV2	0.88	9.18	4.76	0.96	0.1139
PLV3	1.18	9.15	4.73	0.33	0.1392
PLV4	1.48	9.21	4.38	0.00	0.1489

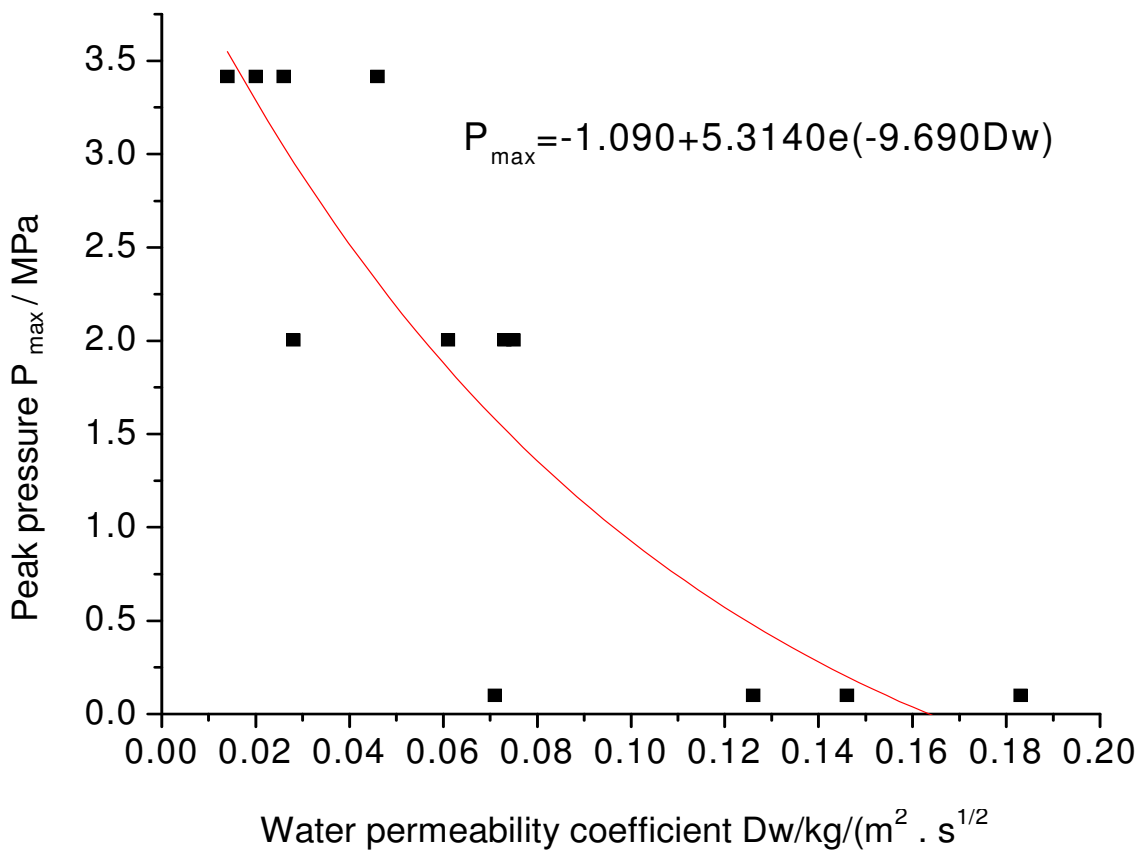


Figure 5. The relationship of peak pore pressure and water permeability coefficient.

$$P_{max} = - 1.090 + 5.314\exp (-9.690Dw) \tag{14}$$

The calculation results are listed in Table 4. Table 4 shows that peak pore pressure in HSC is higher than that in NSC at 600°C. Furthermore, higher strength grades of concrete have higher pore pressure, so the probability of spalling is greater. This indicates that HSC is prone to spalling at high temperature. When polypropylene fibers

are mixed into concrete, the pores pressure decrease. As the quantity of fibers is increased from 0.58 to 1.18 kg/m³, the pore pressure decreases, thus, the probability of spalling is also reduced.

Conclusions

The temperature field and pressure field within concrete

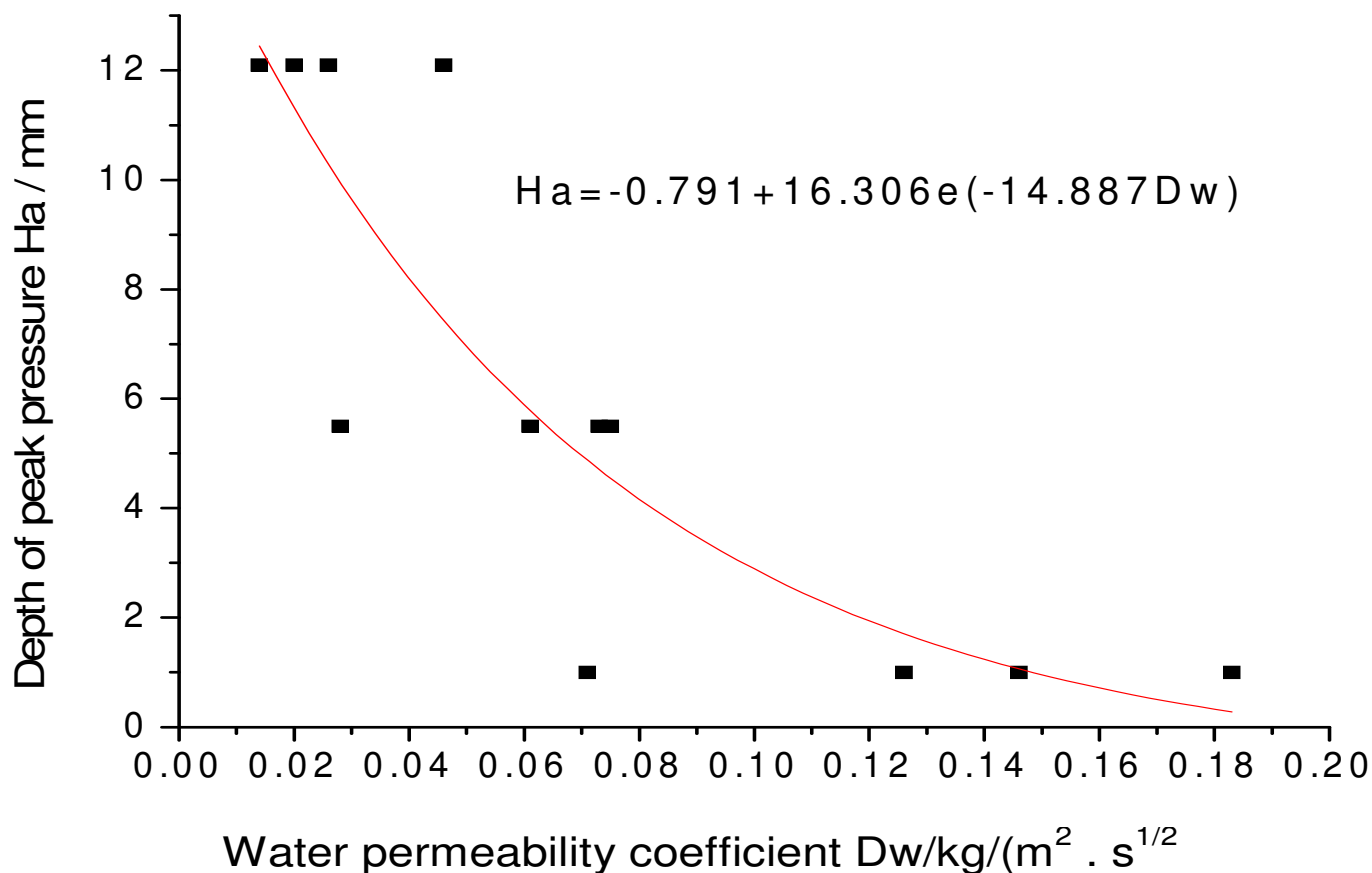


Figure 6. The relationship of depth of peak pore pressure and water permeability coefficient.

Table 4. The pressure of inner pore pressure of concrete at 600°C.

Sample no.	NSC-30	HSC-50	HSC-70	HSC-90	HSC-70PLV1	HSC-70PLV2	HSC-70PLV3
Water permeability coefficient Dw / kg/(m ² ·s ^{1/2})	0.186	0.183	0.146	0.071	0.096	0.113	0.139
Peak pore pressure P _{max} / MPa	1.174	1.280	1.295	2.180	1.720	1.515	1.329

exposed to a given temperature can be calculated from the mathematical model the coupled action of hydrothermal effects established in this paper. Peak pore pressure increases with prolonged fire exposure time, and shifts from the surface towards the center of the concrete. From the calculated results using different empirical formulas for the vapor diffusion coefficient, it can be seen that the peak vapor pressure in pores of concrete decreases after permeability is corrected for the effects of damage caused by high temperatures. The effect of permeability on pore vapor pressure in concrete and the location of the peak pressure can be found through approximation by using the water permeability

coefficient, which is easily measured.

ACKNOWLEDGEMENTS

The authors gratefully acknowledge the financial support for this research from the National Natural Science Foundation of China (50808042) for youths, 11th Five Year Key Program for Science and Technology Development of China (2007BA000875-04), Major State Basic Research Development Program of China (973 Program) (2009CB623203), Research Program for Excellent Young Teachers of Southeast University and

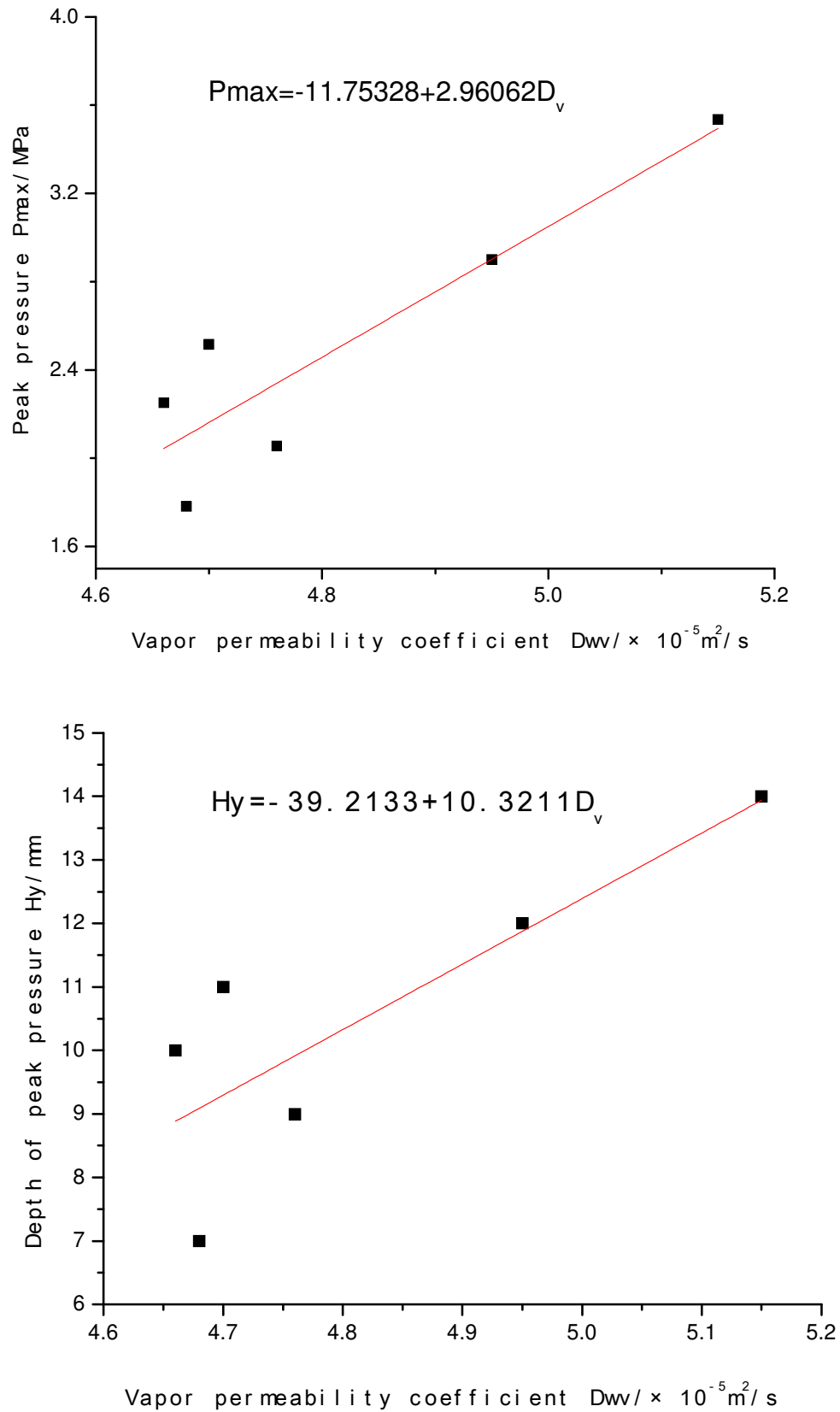


Figure 7. The relationships of vapor permeability coefficient and peak pressure or the depth of peak pressure. (a) The relationship of vapor permeability coefficient and peak pressure. (b) The relationship of vapor permeability coefficient and depth of peak pressure.

Six Projects Sponsoring Talent Summits of Jiangsu Province (1112000053).

REFERENCES

- Aitcin PC (1998). High Performance Concrete. London, England: E&FN SPON Press, p. 591.
- Bazant ZP (1979). Pore Pressure in Heated Concrete Walls: Theoretical Prediction. *Mag. Concrete Res.*, 107: 67-76.
- Cemy R, Rehalova DJ (1996). Methods for evaluation of water-proofness quality and diffusion properties of coating materials. *Const. Building Mat.*, 8: 547-552.
- Ichikawa Y, England GL (2004). Prediction of moisture migration and pore pressure build-up in concrete at high temperatures, *Nuclear Eng. Design*, 228: 245-259.
- Jahren PA (1989). Fire resistance of high strength/dense concrete with particular reference to the use of condensed silica fume, A Review, Detroit, USA: Fly ash ,silica fume, slag, and natural pozzolans in concrete, Proceedings of the Third International Conference, ACISP 114: 1013-1049
- Jean-Christophe M, Pierre P, Albert N, Mulumba K (2010). Temperature, pore pressure and mass variation of concrete subjected to high temperature - Experimental and numerical discussion on spalling risk. *Cement Concrete Res.*, 40(3): 477-487.
- Johannesson BF (2002). Prestudy on diffusion and transient condensation of water vapor in cement mortar. *Cement Concrete Res.*, 32: 955-962 (in Chinese).
- Min L (2005). The fire damage of high temperature concrete and its comprehensive evaluation, PhD dissertation, Southeast University, Nanjing, China.
- Phan LT (1996). Fire Performance of High Strength Concrete: A Report of the State-of -the-Art. NISTIR 5934. Gaithersburg, Maryland: Building and Fire Research Laboratory, Nat. Inst. Standards Technol. p. 105.
- Pieere K, Gregoire C, Chritophe G (2001). High-temperature behavior of HPC with polypropylene fibres from spalling to microstructure. *Cement Concrete Res.*, 31: 1487-1499.
- Van der Heijden GHA, van Bijnen RMW, Pel L, Huinink HP (2007). Moisture transport in heated concrete, as studied by NMR, and its consequences for fire spalling. *Cement Concrete Res.*, 37(6): 894-901
- Wittmann FH, Schweisinger P (1998). High performance concrete-materials peculiarity and design. Translated by FENG Naiqian et al. Beijing: Chinese railway publishing company.
- Yany D, Shen Z (2000). Modeling fully coupled moisture, air and heat transfer in unsaturated soils. *Chin. J. Geotech. Eng.*, 22: 357-361.